Biophysical Chemistry 252 (2019) 106195

Contents lists available at ScienceDirect

Biophysical Chemistry

journal homepage: www.elsevier.com/locate/biophyschem

Calcium(II) oscillations to glucose: An astrocyte relation

Ellen Corcoran[1], Sheryl Hemkin*

Department of Chemistry, Kenyon College, Gambier, OH 43022, USA

HIGHLIGHTS

- Novel mathematical relation linking cytosolic glucose to Ca^{2+} levels
- Model includes spontaneously derived Ca^{2+} activity as well as links to glutamate.
- Analysis of the impact on glucose in response to varying inputs into Ca^{2+} behavior, etc
- Results are consistent with experiment and point toward key mechanistic features.

GRAPHICAL ABSTRACT

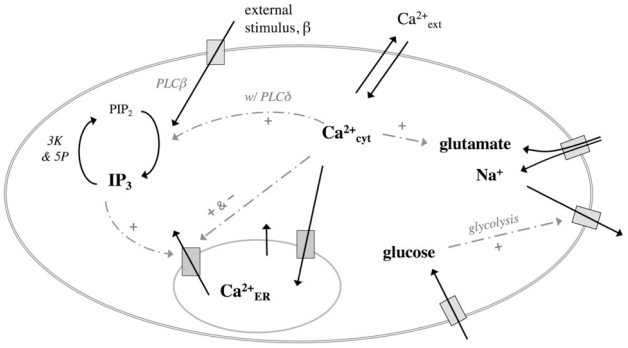

ARTICLE INFO

Keywords:
Astrocyte
Calcium oscillations
Glucose
Metabolism

ABSTRACT

Astrocytes, the most common type of glial cell, are critical to the health of the central nervous system. Evidence implies that changes in the astrocyte's cytosolic calcium concentration is part of a central mechanism by which information is passed and processed in the cell, and it is linked to both external stimuli impacting the cell as well as downstream events such as metabolism and neurotransmitter release. This work proposes a novel chemical model to further the understanding of how extracellular signals could affect intracellular calcium dynamics and metabolic processes within the cell.

1. Introduction

Astrocytes are the most abundant type of glial cell in the brain and are recognized for their multifaceted role within the central nervous system, including evidence that astrocytes help to regulate the synaptic function of neurons, participate in neuronal repair, and maintain immunity of the central nervous system [1]. In the late 1980s it was recognized that while astrocytes did not generate action potentials, they expressed voltage-gated channels, which raised speculation that astrocytes may be actively engaged in neuron-glia interactions [2]. From that point, studies begun to examine whether astrocytes could use their complex chemical signaling pathways to communicate with other cells, like neurons, microglia, and other astrocytes, and thus modulate action in the brain [3].

Calcium (II) commonly plays a role in cellular messaging systems and studies indicates it plays a central role in astrocyte signaling pathways [4,5]. While many parts of this pathway are relatively well understood, e.g. from the binding of the external stimuli by G-protein coupled receptor to cytosolic calcium dynamics, other linkages are not well explored. For example, impaired or dysfunctional astrocytes have been linked to disorders such as epilepsy and neurodegenerative diseases including Amyotrophic Lateral Sclerosis, Parkinson's [6], and

* Corresponding author.
E-mail address: hemkins@kenyon.edu (S. Hemkin).
[1] Present address: Yale University, New Haven, CT 06520.

https://doi.org/10.1016/j.bpc.2019.106195
Received 6 March 2019; Received in revised form 28 May 2019; Accepted 29 May 2019
Available online 30 May 2019
0301-4622/

Alzheimer's [7] Disease. In comparison to healthy astrocytes, these cells have often undergone functional and morphological changes, including changes in the typical frequency of oscillations of the cytosolic Ca^{2+} concentration, metabolic changes, etc. Additionally, in studies of epilepsy [8] and Alzheimer's [7], astrocytes are implicated in disrupting neuron energy homeostasis via their own impacted metabolic pathways. Studies such as these infer that calcium oscillations and metabolism are inter-connected within an astrocyte. Coupled with the knowledge that astrocytes are able to respond to external stimuli through downstream changes in the cytosolic Ca^{2+} levels and subsequent release neurotransmitters [9,10], a large network of connection is implied. Furthermore, due to the astrocyte's physical proximity to the synapse, it is postulated that astrocytes have the ability to mediate qualities like synapse health and neuronal information transfer [11]. Thus, knowledge of the cytosolic Ca^{2+} mechanism and its connectivity, particularly toward metabolic pathways, can give insight into the health of the astrocyte and the central nervous system.

The goal of this work is to contribute to the understanding of the mechanism by which cytosolic calcium and glucose are linked. A variety of studies characterize the behavior of calcium and its relationship with IP_3 [12–14] and there are a number of studies that connect cytosolic calcium with compounds that could serve as intermediaries [15–17] (e.g. glutamate) in a putative mechanism that joins to glucose, but there is a dearth of information as to how these intermediate compounds intersect. In this paper we present a model, that produces experimentally relevant results, that extends and connects previous models and experimental evidence to give mechanistic insight as to how external stimuli (via G-protein coupled receptors) and calcium behavior can influence glucose levels (which feeds into the metabolic pathways).

2. Methods and materials

Numerical integrations were performed using Mathematica and Berkeley Madonna (ver. 9.1.9) a differential equation solver with a suite of integration algorithms. In particular, the Rosenbrock algorithm was utilized.

3. Mathematical model

We develop our study in two parts, the formation of a core model involving cytosolic Ca^{2+} and then the extension of that model to include glucose, a primary component of metabolism. The construction of the model "core" allows for the spontaneous formation of Ca^{2+} oscillations, an observed process that is not often included in such models, as well as for the formation of oscillations prompted by extracellular signaling that activates IP_3 production. In the second part, the model is extended to include a mechanistic path between cytosolic Ca^{2+} and glucose. While there is experimental evidence of this relationship, it studied segmentally and not as whole entity, thus this unifying model lends insight as to how external chemical signals such as glutamate can perturb baseline calcium oscillations and this in turn can affect glucose concentration and thus, metabolism.

3.1. Model core

The core of the model supports both spontaneously generated oscillations and those triggered by external chemical stimulation. In the simulation, spontaneous oscillatory behavior is initiated by the influx of calcium from the extracellular space into the cytosol. This agrees with experimental data indicating that significant changes in the cytosolic calcium concentration can result from small changes in the influx of extracellular calcium into the cell [18–20]. This oscillatory mode has been observed in *in vitro* and *in situ* experiments where there are no neurons nor external stimuli, like glutamate, present in the extracellular medium. In contrast, externally stimulated oscillations resulting from the binding of signal molecules such as ATP or glutamate to receptors in the astrocyte's membrane, and our simulations also mimic this scenario [21]. Overall, this model allows for the promotion of the oscillatory behavior through different paths (spontaneously and externally provoked), which can work in conjunction *in vivo*.

The core of the model (Supplemental Fig. 1) tracks the concentrations of three key chemical species using ordinary differential equations, (ODEs); calcium ions in the cytosol, (Ca_{cyt}^{2+}, Eq. (1)), calcium ions in the endoplasmic reticulum, the main calcium store in the cells, (Ca_{ER}^{2+}, Eq. (2)), and inositol trisphosphate in the cytosol (IP_3, Eq. (3)). A fourth variable is also described, a gating variable, (h, Eq. (4)), that relates to the fraction of active IP_3 receptors on the endoplasmic reticulum (ER) membrane, and this is employed within the detailed description of the both the calcium ion concentrations (Eqs. (1) and (2)).

Abbreviated equations for the model core:

$$\frac{d[Ca^{2+}]_{cyt}}{dt} = \nu_{in} + \nu_{CICR} + k_f([Ca^{2+}]_{ER} - [Ca^{2+}]_{cyt}) - \nu_{serca} - k_{out}[Ca^{2+}]_{cyt} \quad (1)$$

$$\frac{d[Ca^{2+}]_{ER}}{dt} = \nu_{serca} - \nu_{CICR} - k_f([Ca^{2+}]_{ER} - [Ca^{2+}]_{cyt}) \quad (2)$$

$$\frac{d[IP_3]}{dt} = \nu_{plc\delta} + \nu_{plc\beta} - \nu_{5P} - \nu_{3K} \quad (3)$$

$$\frac{d(h)}{dt} = \frac{h_\infty - h}{t_h} \quad (4)$$

3.1.1. Ca^{2+} in the cytosol

In this model, the concentration of Ca^{2+} in the cytosol (Eq. (1)) depends on five significant transport processes that occur within the astrocyte. Three transport pathways bring Ca^{2+} into the cytosol and two paths remove it, with the extracellular solution and the endoplasmic reticulum, being important sources and sinks.

The term ν_{in} represents the Ca^{2+} flow from the extracellular medium through the membrane to the cytosol. This influx is essential to initiate and sustain spontaneous oscillatory behavior in most tissues and is supported by experimental data that shows the spontaneous oscillations are virtually eliminated when cultured astrocytes are placed in a calcium free medium or bathed in a non-specific voltage gated Ca channel blocker [18,22].

This model also considers two transport processes that allow Ca^{2+} to flow into the cytosol from the endoplasmic reticulum (ER), and both are driven by diffusion. The endoplasmic reticulum is the largest dynamic calcium store in the cell and it is capable of accumulating, storing, and releasing calcium in response to physiological stimulation. (The mitochondria are also a significant stores of calcium, but their entry mechanism, the calcium uniporter, has a much lower affinity for calcium than the endoplasmic reticulum's SERCA pump and thus is not considered in this work.) One of the diffusion-based pathways, $k_f([Ca^{2+}]_{ER} - [Ca^{2+}]_{cyt})$, is a passive leak flux and it involves calcium passively diffusing through unactivated IP_3 receptors [22]. The second pathway, involves the diffusion of Ca^{2+} through open and activated IP_3 receptors. This has been called calcium-induced calcium release (CICR) and is represented in this model as v_{CICR} (in Eqs. (1) and (2)), which expands as [23],

$\nu_{CICR} = \nu_{M3} m_\infty^3 n_\infty^3 h^3 ([Ca^{2+}]_{ER} - [Ca^{2+}]_{cyt})$ and h is derived from Eq. (4): $\frac{d(h)}{dt} = \frac{h_\infty - h}{t_h}$

where: $m_\infty = \left(\frac{[IP_3]}{[IP_3] + d_1}\right)$, $n_\infty = \frac{[Ca^{2+}]_{cyt}}{[Ca^{2+}]_{cyt} + d_5}$,

$h_\infty = \frac{Q_2}{Q_2 + [Ca^{2+}]_{cyt}}$, $Q_2 = d_2 * \frac{[IP_3] + d_1}{[IP_3] + d_3}$, $t_h = \frac{1}{a_2(Q_2 + [Ca^{2+}]_{cyt})}$.

This process allows for a gated, diffusion-driven release of calcium from ER stores via the IP_3 receptor and results in an increase in calcium levels in the cytosol. The flow is regulated by the concentration of IP_3

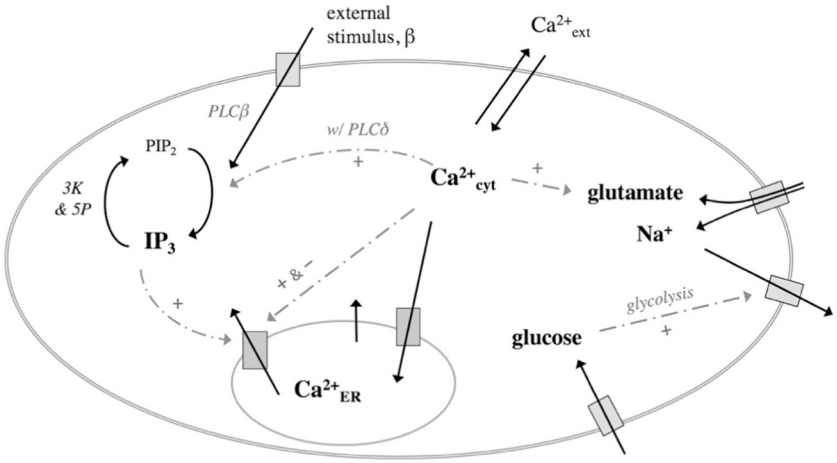

Fig. 1. Schematic illustration of extended model. The core of the model allows for cytosolic Ca^{2+} oscillations to be prompted by extracellular stimuli like ATP, etc., as well as to be generated spontaneously, i.e. arise from calcium flux from the extracellular space. The model utilizes one internal Ca^{2+} store, the endoplasmic reticulum (ER), and IP_3 is produced via pathways associated with the enzyme PLCδ or PLCβ. To extend the model toward metabolism, flows involving glutamate, Na^+ ion, and glucose are also included. The dashed lines indicate feedback or cooperative effects.

and Ca^{2+} in the cytosol and both species have binding sites on the receptor. The binding of IP_3 helps to open the channel, whereas the binding of calcium ions allows for both a positive and negative effect on the activity of the channel due to a higher and lower affinity binding site, respectively [23]. In consequence, the regulated transport through the IP_3 receptor has a bell-shaped dependence on the concentration of Ca^{2+} in the cytosol, which is in accordance with experiment [24].

There are two transport processes that serve to decrease Ca^{2+} in the cytosol, one transfers Ca^{2+} to the extracellular solution and the other process stores the Ca^{2+} in the ER. In the first process, the rate of efflux to the extracellular, k_{out}*$[Ca^{2+}]_{cyt}$, is dependent on the concentration of calcium in the cytosol [25]. The second process involves the endoplasmic reticulum (ER) and its sarco/endoplasmic reticulum Ca^{2+}-ATPase (SERCA) pump, which actively moves the ions from the cytosol to the ER [26].

$$\nu serca = \nu_{M2}\frac{[Ca^{2+}]^2_{cyt}}{[Ca^{2+}]^2_{cyt} + k_2^2}$$

3.1.2. Ca^{2+} in the endoplasmic reticulum

The concentration of Ca^{2+} in the ER (Eq. (2)) depends on three transport processes that allow for the movement of Ca^{2+} to and from the cytosol. These processes mirror three of those proposed for Ca^{2+} in the cytosol; the activation of the SERCA pump and IP_3 receptor, as well as the diffusive leak out of the ER.

3.1.3. IP_3 in the cytosol

The inositol trisphosphate (IP_3) concentration in the cytosol is based on two production and two degradation routes. The formation of IP_3 (and diacylglyceride, DAG) results from the hydrolysis of the membrane bound lipid phosphatidylinositol 4,5-bisphosphate (PIP_2). This reaction is catalyzed by isozymes of phospholipase C (PLC), with the β- and δ-versions providing for two different IP_3 production paths in this model [27]. The degradation of IP_3 is characterized by two pathways each involving a different enzyme, either inositol polyphosphate 5-phosphatase or IP_3 3-kinase.

The IP_3 production route associated with spontaneously generated oscillations must be initiated by a mechanism internal to the cell. This path involves the PLCδ isozyme and is activated by increased cytosolic calcium levels thus it provides a positive feedback loop between cytosolic Ca^{2+} and IP_3 [28]

$$\nu_{plc\delta} = \nu_7\frac{[Ca^{2+}]^2_{cyt}}{K^2_{cax} + [Ca^{2+}]^2_{cyt}}$$

The activation of the PLCβ pathway is controlled by external stimuli binding to G-protein coupled receptors on the cell membrane. The rate at which PLCβ produces IP_3 is expressed by the equation [29]:

$$\nu_{plc\beta} = \nu_8\, a_0\, [(1 + k_g) * (k_g/(1 + k_g) + a_0)]^{-1}$$

The term assumes the ligand concentration will be saturating and k_g represents the ratio of the G-protein/PLCβ dissociation constant to the total concentration of G-protein, while a_0 indicates the ratio of the total concentration of agonist receptors to the G-protein/agonist dissociation constant.

Two significant degradation pathways of IP_3 have been observed. One established route is IP_3 dephosphorylation via the enzyme inositol polyphosphate 5-phosphatase (IP-5P), and the second is via IP_3 phosphorylation by the IP_3 3-kinase (IP_3-3 k) which is calcium dependent [27,30].

$$\nu_{5P} = k_{5P}\,[IP_3]\;\nu_{3K} = k_{3K}\left(\frac{[Ca^{2+}]^4_{cyt}}{[Ca^{2+}]^4_{cyt} + K_d^4}\right)\left(\frac{[IP_3]}{[IP_3] + K_3}\right)$$

3.2. Extension to glucose and influence on metabolism

The system, as modeled to this point, can be regarded as an information processing unit; external stimulation can influence the oscillatory behavior of the cytosolic Ca^{2+} and, in turn, it appears to influence the release of chemical species such as neurotransmitters that are relevant to intercellular signaling. In addition to those interactions already noted, we also postulate that Ca^{2+} can indirectly affect glucose levels [31]. The experiment based logic for the calcium-glucose connection starts with the observation that cytosolic Ca^{2+} oscillations indirectly modulate the concentration of glutamate in the astrocyte [32]. While there are additional mechanisms by which the glutamate concentration in the cell is regulated (ex. via glutamine formation), it is at least partially influenced by Ca^{2+} in the cytosol. Additionally, the increase in glutamate – which is naturally accompanied by an inflow of Na^+ – corresponds to the activation of the Na^+/K^+-ATPase (sodium-potassium pump), which will return the growing excess of Na^+ in the cytosol back to the extracellular solution. Studies indicates that activation of this pump prompts glucose uptake and glycolysis, likely to provide ATP to power this transport process [33]. (Fig. 1.) Taken overall, the experiments indicate a relationship between calcium ions in the cytosol and metabolism that has not been well explored as a whole.

The model's expansion to connect Ca^{2+} oscillations with glucose influx adds four variables implied by the linkage: glutamate in the cytosol ($[glutamate]_{cyt}$, Eq. (5)), flux of glutamate into the cytosol (*glutamate_flux*, Eq. (6)), Na^+ in the cytosol ($[Na^+]_{cyt}$, Eq. (7)), and glucose in the cytosol ($[glucose]_{cyt}$, Eq. (8)).

Abbreviated equations for the model extension:

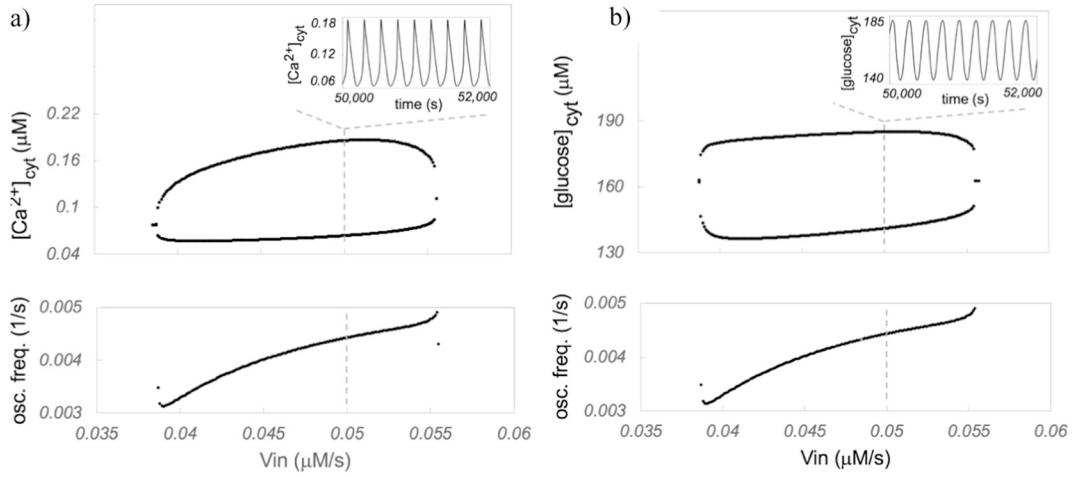

Fig. 2. Development of oscillatory behavior under spontaneous conditions. Oscillations in the concentrations of cytosolic calcium ions and glucose are developed at certain levels of constant Ca^{2+} influx (ν_{in}) from the extracellular solution into the cytosol. Inflow rates that generate oscillatory behavior lie in the range of 0.03–0.06 M s^{-1}. a.) *Upper panel:* Bifurcation diagram showing the maximum and minimum cytosolic calcium concentration in the oscillatory range (upper and lower trace, respectively). *Inset*: Time series at $\nu_{in} = 0.05$. *Lower panel:* Frequency of oscillations in Ca^{2+}. b.) *Upper panel:* The inflow also stimulates oscillations in glucose. Bifurcation diagram showing the maximum and minimum cytosolic glucose concentration in the oscillatory range. *Inset:* Time series at $\nu_{in} = 0.05$ *Lower panel:* Frequency of oscillations in glucose.
Initial conditions: $[Ca^{2+}]_{cyt} = 0.3\,\mu M$, $[Ca^{2+}]_{ER} = 1.4\,\mu M$, $[IP_3]_{cyt} = 0.13\,\mu M$, $h = 0.8\,\mu M\,s^{-1}$, $[glutamate]_{cyt} = 3000\,\mu M$, *glutamate_flux* $= 0.0387\,\mu M\,s^{-1}$, $[Na^+]_{cyt} = 400\,\mu M$, $[glucose]_{cyt} = 400\,\mu M$, $\nu_{plc\beta}$ *scaling/stimulus variable* $(\beta) = 0$. *Other parameters as listed in* Table 1.

$$\frac{d[glutamate]_{cyt}}{dt} = \nu_{glut\_in} - \nu_{glut\_out} \quad (5)$$

$$\frac{d(glutamate\_flux)}{dt} = \nu_{glt\text{-}1} + \nu_{glast} \quad (6)$$

$$\frac{[Na^+]_{cyt}}{dt} = \nu_{glut\text{-}na} - \nu_{sod} \quad (7)$$

$$\frac{[glucose]_{cyt}}{dt} = \nu_{gluc} + \nu_{gluc\text{-}GLUT} - \nu_{nak} \quad (8)$$

3.2.1. Glutamate in the cytosol

In this model, the regulation of cytosolic glutamate serves as a link between Ca^{2+} and glucose. Glutamate, a common signaling molecule, is regularly taken into the astrocyte to aid in the maintenance of proper extracellular concentrations [15]. This influx of glutamate must be managed by the astrocyte, and while there are a variety of pathways that will decrease the internal glutamate concentration (ex. conversion to glutamine), this reduced model only considers a Ca^{2+} dependent path, $\nu_{glut\_in} = k_4$ *(glutamate_flux). There is strong evidence that elevation of cytosolic Ca^{2+} induces the reduction of glutamate concentration in the cytosol, and studies indicate this results from a vesicular glutamate transporter (VGLUT) mediated release [34] which depends on both calcium and glutamate levels, $\nu_{glut\_out} = k_{15} * [Ca^{2+}]_{cyt} * [glutamate]_{cyt}$.

3.2.2. Glutamate influx

The glutamate influx represents the rate of glutamate transport into the cytosol from the extracellular solution, and there are two major transport processes for this. Studies show that astrocytic glutamate uptake from the extracellular solution is accomplished by two transporters, GLT-1 and GLAST (also known as EAAT2 and EAAT1, respectively), that rely on the sodium diffusion in to the cell to drive the glutamate against its concentration gradient [16].

$$\nu_{glt-1} + \nu_{glast} = (k_7 * GLT + k_8 * GLAST) * (k_{16} * [Na^+]_{ext} - [Na^+]_{cyt})$$

3.2.3. Sodium in the cytosol

As noted previously, glutamate transporters couple glutamate and Na^+ movement. Consequently, the Na^+ concentration in the cytosol (Eq. (7)) is modeled by two processes, an influx resulting from glutamate co-transport, and an efflux due to the cell's maintenance of the Na^+ gradient across the membrane via the sodium-potassium pump (Na^+/K^+–ATPase) [15,17].

$$\nu_{glut\text{-}na} = k_{10} * [glutamate]_{cyt} \quad \nu_{sod} = k_{14} * [Na^+]_{cyt}$$

3.2.4. Glucose in the cytosol

Several research groups have provided strong evidence that glutamate uptake (and its co-transport of Na^+) into the cytosol indirectly activates glucose influx and subsequently, glycolysis [17]. In this model, glucose is modeled by two influx paths and the loss of glucose into glycolysis, the first stage of metabolism. Glucose influx from extracellular space is indirectly stimulated by the amount of glutamate in the cytosol, $\nu_{gluc} = k_1 * [glutamate]_{cyt}$, and uptake through the glucose specific transporter, GLUT-1 is represented by $\nu_{gluc\text{-}GLUT} = k_{2a} * [glucose]_{cyt}$ [35]. Glucose is lost to glycolysis, the first stage of metabolism and is represented by $\nu_{nak} = k_{3a} * nak * [glucose]_{cyt}$ [35]. Experiment indicates that an upregulation in glycolysis follows the activation of the sodium-potassium pump, which requires ATP to facilitate the removal of Na^+ ions co-transported with glutamate [33]. Additionally, this metabolic activation may also have energy ramifications for the neuron; some groups postulate that lactate, a potential downstream product of glycolysis, can be shuttled to the neuron and used as an additional energy source [36].

4. Results & discussion

4.1. Core of model

In solutions devoid of extracellular messengers, such as ATP and glutamate, astrocytes can still exhibit oscillations (as in *in situ* environments). Evidence indicates these oscillations arise from the influx of Ca^{2+} from the extracellular medium since they can be abolished when the study is conducted in Ca^{2+} free-medium [20]. To test the model's ability to simulate this behavior, the influx of Ca^{2+} from the extracellular to the cytosol is manipulated through the value of v_{in} (Eq. (1)) and the degree of extracellular stimulation (embedded in Eq. (3)) is

terminated by multiplying $\nu_{plc\beta}$ by a scaling or stimulus variable (β) set to zero. As v_{in} is raised from zero (no Ca^{2+} influx), the behavior of the model system moves from steady state to period-one oscillations and then back to steady state at the higher inflow rates. (Fig. 2a). Extending the model to glucose, a similar response is seen indicating that the behavior of calcium in the cytosol can influence the concentration glucose, the chemical start of glycolysis. (Fig. 2b).

These simulations also produce spontaneous oscillations in the cytosolic Ca^{2+} concentration that have a shape, amplitude and frequency similar to that seen in experiment In the spontaneous region, as the v_{in} increases there is an increase in oscillatory frequency, which has been seen experimentally [22]. Other models of calcium ion behavior have uncovered more exotic oscillatory behavior [37], however the behavior seen in these simulations bears relation to published laboratory work. The frequency of oscillation, which corresponds to a period that varies between approximately 210–320 s, is characteristic of the relatively slow dynamics seen in most spontaneous activity (on the order of 100 s) [22]. (Fig. 2a, lower panel) Experimentally, oscillations do not occur with perfect regularity as seen in the simulations, however this is likely due to the minimalist roots of the model and the lack of any stochastic process in the postulated mechanism. That said, the period-1 behavior of Fig. 2a has qualitative agreement with experimental results from epileptiform tissues [38].

The endoplasmic reticulum has long been thought to play a significant role in the oscillatory process due to its ability to quickly store and release large quantities of Ca^{2+} ions. Experimental inhibition of the SERCA pump by thapsigargin shows a decrease in both the amplitude and frequency of the cytosolic Ca^{2+} oscillations [20]. Additionally, the experimental use of SERCA pump inhibitor cyclopiazonic acid also leads to a large reduction in the number of cells with spontaneous oscillatory behavior [18]. To mimic the inhibition of the pump in simulations, the parameter controlling the maximum flow rate through the SERCA pump, v_{M2}, was decreased. In contrast to experiment, the frequency increases in the simulations and this is thought to be a product of the minimalist model. In parallel to experimental results, however, as the flow rate is lowered the model shows the oscillatory amplitude is reduced, and at very low v_{M2} values, steady state behavior is seen. (Supplemental Fig. 2a).

The IP_3 receptor allows for the release of Ca^{2+} from the endoplasmic reticulum. Experimentally, the inhibition of the IP_3 receptor by heparin or 2-aminoethoxydiphenylborate (2-APB) reduced Ca^{2+} oscillations [22]. Simulation of this inhibition is accomplished by decreasing v_{M3}. Similar to experiment, this results in a decrease in oscillatory amplitude and frequency, until steady state develops at very low values. (Supplemental Fig. 2b)

This model also allows for the introduction of an external stimulus (ex. ATP or glutamate) that can influence the oscillatory process by perturbing IP_3 production mediated by PLCβ. Experimentally, addition of a glutamate receptor agonist increases the frequency of the $[Ca^{2+}]_{cyt}$ [39]. To simulate varying levels of an external stimulus, the PLCβ-mediated IP_3 production term in Eq. (3) is multiplied by a scaling variable (β) with the allowed values of 0–1, which indicate the relative level of stimulation. In the oscillatory range of the model, as external stimulation (β) is reduced, the frequency of the oscillations decreases in accordance with experiment, however the average concentration of Ca^{2+}_{cyt} increases (but remains in the physiological range). (Fig. 3a) In extending the model to glucose, a similar response is seen, again indicating that the behavior of calcium in the cytosol can influence the concentration glucose which is a key species in metabolism (Fig. 3b)

4.2. Extended model

To gain insight on the experimental links between cytosolic Ca^{2+} and metabolism, our core model was extended using empirically derived links between $[Ca^{2+}]_{cyt}$ and $[glucose]_{cyt}$, the key chemical entry point into metabolism. The values found in Table 1 are tuned to keep the species involved in the model in the physiological range. With two exceptions this was accomplished; the species that fall outside of the range are the cytosolic concentration of Na^+ and the influx of glutamate across the cell membrane. The simulated cytosolic sodium level (~4 mM) is on par for cells such as neurons, however astrocytes operate with a higher concentration (~15-20 mM) [40]. This indicates our reduced model is missing some detail within this part of the mechanism. That said, the concentrations of Ca^{2+} and glucose in the cytosol are physiologically relevant and thus this work can provide insight into the linkage at this stage of investigation.

Early experiments with astrocytes indicated that glutamate uptake resulted in glucose influx and metabolic upregulation [17]. To examine the effect of glutamate influx on glucose transport, the coefficient of the glutamate flux term, k_4, was varied. In accordance with experiment, simulations show that the concentration of glucose in the cytosol increases in a sigmoidal fashion with the rate of glutamate influx [33]. (Fig. 4)

Another well studied relationship is the co-transport of glutamate with sodium ions. Experimentally, when astrocytes are incubated in Na^+-free medium the glutamate-stimulated increase in glucose uptake is abolished [17]. Like in the experiment, the simulation shows inhibition of glutamate-stimulated glucose uptake when the concentration of extracellular Na^+ is set equal to zero. (Supplemental Fig. 3)

Observations also show that the inhibition of the glutamate transporters affects the concentration of cytosolic Na^+ (and glucose uptake) but not Ca^{2+}, that is, the sodium pathway appears to be downstream of the Ca^{2+} inputs. Experimentally, this was seen in the significant inhibition of Na^+ waves using TBOA, a glutamate transport inhibitor, and the lack of effect on the Ca^{2+} behavior [31]. Similar results were seen when the astrocyte was examined in extracellular medium that contained an modified version of glutamate (e.g. 2-oxoglutarate) which is not transported into the cell as efficiently [31]. A parallel examination with this model involves controlling the contribution from the GLT-1 and GLAST transport process by multiplying a scaling parameter into Eq. (6). (That is, the contribution from each transport process was modulated by the same value.) Similar to experiment, when the scale value is set to zero the glutamate transporters are effectively inhibited and $[Na^+]_{cyt}$ falls to approximately zero, however no change is observed in the simulation of cytosolic calcium. (Supplemental Fig. 4, black and grey trace respectively) Additionally, the model also shows a maximal concentration of sodium which parallels the effect in cells [40].

Studies also show that activation of the sodium-potassium pump of the Na^+/K^+-ATPase stimulates glycolysis [17]. The active transport of Na^+ out of the cell through these pumps is an energy consuming process, thus the rate of glycolysis is increased in order to provide ATP for the process. Experimental work with ouabain, a Na^+/K^+-ATPase inhibitor, found that inhibition of this pump reduces the downstream glucose uptake [17], and our model agrees with this result. In the model, the fraction of activated Na^+/K^+-ATPase pumps was modulated via the term nak (Eq. (8)), and with increasing activation, simulation shows a concurrent depletion of glucose, which would correspond to the upregulation of glycolysis. (Fig. 5)

5. Conclusion

This study is a novel endeavor to model the experimentally indicated connection between the astrocyte's cytosolic calcium ion oscillations and astrocyte metabolism, and this work shows there is a plausible chemical link between the behavior of the calcium in the cytosol and the concentration of glucose in the cell. As indicated in the results section, the development of this reduced model was informed by laboratory studies that show intermediate linkages between the astrocyte's cytosolic calcium ion concentration and glycolysis, and this work shows positive correlations between simulation and laboratory results. These studies indicate that glucose concentration and metabolism in the

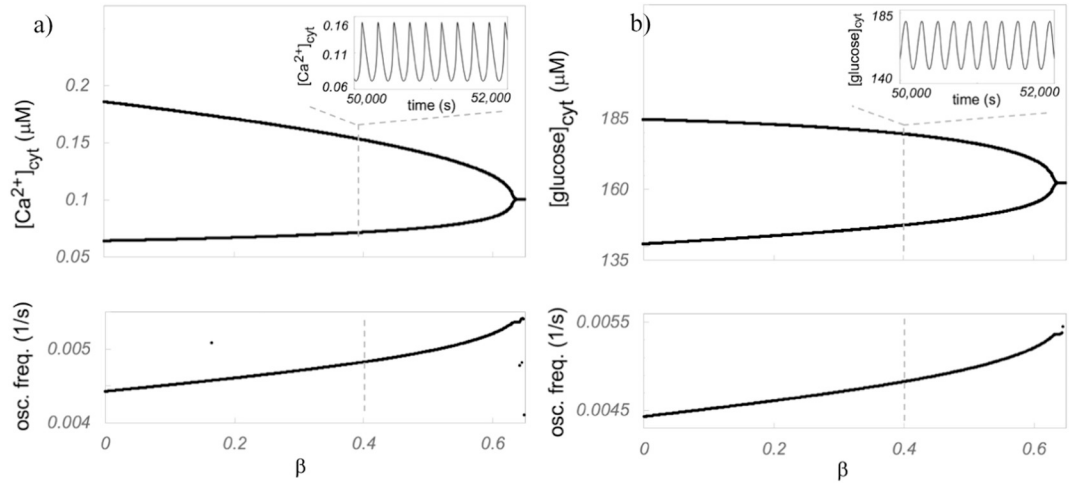

Fig. 3. Oscillatory behavior varies with the degree of external stimulation to the cell. Oscillations in the concentration of calcium ions and glucose resulting from spontaneous and external stimulation (β), for example, from ATP binding. a.) *Upper panel:* Bifurcation diagram showing the maximum and minimum cytosolic calcium concentration in the oscillatory range (upper and lower trace, respectively). *Inset:* Time series at β = 0.4 *Lower panel:* Frequency of oscillations in Ca^{2+}. b.) *Upper panel:* Resulting oscillations in glucose. Bifurcation diagram showing the maximum and minimum cytosolic glucose concentration in the oscillatory range. *Inset:* Time series at β = 0.4 *Upper panel:* Frequency of oscillations in glucose.
Initial conditions: $[Ca^{2+}]_{cyt} = 0.3\,\mu M$, $[Ca^{2+}]_{ER} = 1.4\,\mu M$, $[IP_3]_{cyt} = 0.13\,\mu M$, $h = 0.8\,\mu M\,s^{-1}$, $[glutamate]_{cyt} = 3000\,\mu M$, $glutamate\_flux = 0.0387\,\mu M\,s^{-1}$, $[Na^+]_{cyt} = 400\,\mu M$, $[glucose]_{cyt} = 400\,\mu M$. *Other parameters as listed in* Table 1.

astrocyte can be influenced by cytosolic calcium levels, thus, extracellular signals and/or internal events that alter the calcium ion behavior is of import. That is, this work suggests that metabolism may have important upstream trigger points, both internal and external to the astrocyte, and that deviations from the norm may cause dysfunction in the astrocyte's energy flow that can disrupt the astrocyte's normal function and influence neighboring cells, including neurons, as well as certain pathological conditions.

Table 1
Glossary of parameters).

Parameter	Description	Value	Reference
v_{in}	Influx of calcium from the extracellular medium	0.05 μM s^{-1}	[29]
v_{M2}	Maximal flow of Ca^{2+} out of the SERCA pump	6 μM s^{-1}	[24]
v_{M3}	Maximal CICR Ca^{2+} flow rate	6 s^{-1}	[23,26]
v_7	Maximal rate of IP_3 production by PLCδ	0.05 μM s^{-1}	[29]
v_8	Maximal rate of IP_3 production by PLCβ	1 μM s^{-1}	[29]
d_1	IP_3R – IP_3 dissociation constant	0.13 μM	[26]
d_2	IP_3R – Ca^{2+} dissociation constant (inhibition)	1.049 μM	[26]
d_3	IP_3R – IP_3 dissociation constant	0.9434 μM	[26]
d_5	IP_3R – Ca^{2+} dissociation constant (activation)	0.08234 μM	[26]
k_f	Maximal rate of calcium leakage through unactivated IP_3 receptors	0.5 s^{-1}	[26]
k_{out}	Rate constant calcium efflux from the cytosol into the extracellular medium	0.5 s^{-1}	[29]
k_g	Ratio of the dissociation constant for G-protein binding to PLCβ to the total concentration of G-protein	1	[29]
k_1	Rate constant of glutamate-stimulated glucose flux	0.0003 s^{-1}	[35]
k_2	Half-maximal value effect of the SERCA affinity	0.1 μM	[41,42]
k_{2a}	Rate constant affiliated with glucose influx through glucose transporter	0.0003 s^{-1}	[35]
k_{3a}	Rate constant associated with Na^+/K^+ -ATPase	0.0100 s^{-1}	[35]
k_{3k}	Maximal rate of IP_3 degradation by IP_3-3K	2 μM s^{-1}	[43]
k_4	Glutamate flux constant	0.01	[35]
k_{5p}	Maximal rate of IP_3 degradation by IP-5P	0.04 s^{-1}	[43]
k_7	GLT-1 rate constant	0.1 s^{-1}	[35]
k_8	GLAST rate constant	0.01 s^{-1}	[35]
k_{10}	Rate constant of sodium entering cytosol	0.1 s^{-1}	[35]
k_{14}	Rate constant of sodium leaving cytosol	0.1 s^{-1}	[35]
k_{15}	Rate constant of glutamate removal from cytosol	1.0 μM^{-1} s^{-1}	[35]
k_{16}	Na^+ gradient modulation	0.03	
a_o	Ratio of the total concentration of agonist receptors to the dissociation constant for receptor binding to G-protein	0.001	[29]
a_2	IP_3R – Ca^{2+} binding constant (inhibition)	0.2 (μM s)$^{-1}$	[26]
K_{cax}	PLCδ – Ca^{2+} dissociation constant	0.3 μM	[29]
K_d	Ca^{2+} affinity of IP_3-3k	0.7 μM	[30,43]
K_3	IP_3 affinity of IP_3-3k	1 μM	[43]
nak	Fraction of Na^+/K^+ -ATPase pumps activated	1	[35]
GLT	Fraction of GLT-1 transporters available	0.1	[35]
GLAST	Fraction of GLAST transporters available	0.1	[35]
$[Na^+]_{ext}$	Concentration of external sodium	17,500 μM	[40]
β	Scaling (or Stimulus) Factor for value for $v_{plcβ}$	0 -1	

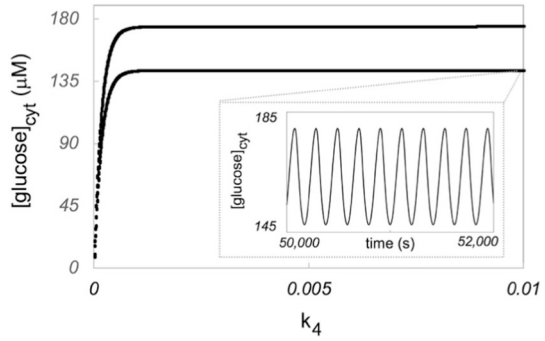

Fig. 4. Glutamate uptake triggers glucose influx. An increase in glutamate uptake was followed by an increase in glucose influx. Larger values of k_4 correspond to a larger capacity for glutamate transport through the cell membrane. The maximum and minimum glucose concentration in the oscillatory range is illustrated with the upper and lower trace, respectively. Inset: Time series at $k_4 = 0.01$.
Initial conditions: $[Ca^{2+}]_{cyt} = 0.3\,\mu M$, $[Ca^{2+}]_{ER} = 1.4\,\mu M$, $[IP_3]_{cyt} = 0.13\,\mu M$, $h = 0.8\,\mu M\,s^{-1}$, $[glutamate]_{cyt} = 3000\,\mu M$, *glutamate flux* $= 0.0387\,\mu M\,s^{-1}$, $[Na^+]_{cyt} = 400\,\mu M$, $[glucose]_{cyt} = 400\,\mu M$. *To work within the system's oscillatory range, the value β was set to 0.4. Other parameters as listed in* Table 1.

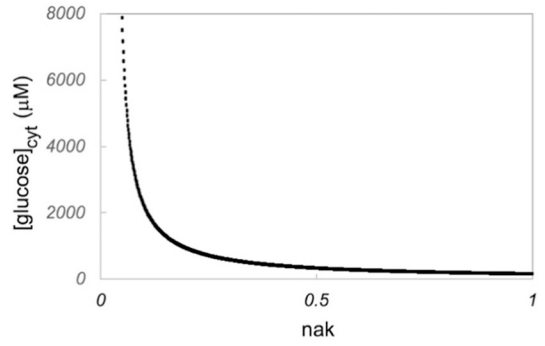

Fig. 5. The sodium-potassium pump activates glucose consumption. A decrease in the concentration of glucose in the cytosol was prompted by the activation of the Na^+/K^+-ATPase pumps which expel Na + from the cell in an ATP dependent manner. Larger values of *nak* correspond to a larger efflux of Na + from the cell, and this happens in conjunction with an increase ATP utilization, which is a product of glycolysis and glucose consumption. The maximum and minimum glucose concentration in the oscillatory range is illustrated with the upper and lower trace, respectively.
Initial conditions: $[Ca^{2+}]_{cyt} = 0.3\,\mu M$, $[Ca^{2+}]_{ER} = 1.4\,\mu M$, $[IP_3]_{cyt} = 0.13\,\mu M$, $h = 0.8\,\mu M\,s^{-1}$, $[glutamate]_{cyt} = 3000\,\mu M$, *glutamate flux* $= 0.0387\,\mu M\,s^{-1}$, $[Na^+]_{cyt} = 400\,\mu M$, $[glucose]_{cyt} = 400\,\mu M$. *To work within the system's oscillatory range, the value β was set to 0.4. Other parameters as listed in* Table 1.

Acknowledgements

We are grateful to Rayan Abboud for his Excel programming.

Funding

We are grateful to the Kenyon College Summer Science program for support of EC.

Competing interests

The authors have no competing interests.

Appendix A. Supplementary data

Supplementary data to this article can be found online at https://doi.org/10.1016/j.bpc.2019.106195.

References

[1] K.M. Lee, A.G. MacLean, New advances on glial activation in health and disease, World J. Virol. 4 (2) (2015) 42–55.
[2] A. Verkhratsky, Patching the glia reveals the functional organisation of the brain, Cell. Neurophysiol. 453 (3) (2006) 411–420.
[3] B.S. Khakh, M.V. Sofroniew, Diversity of astrocyte functions and phenotypes in neural circuits, Nat. Neurosci. 18 (7) (2015) 942–952.
[4] M.J. Berridge, P. Lipp, M.D. Bootman, The versatility and universality of calcium signaling, Nat. Rev. Mol. Cell Biol. 1 (October) (2000) 11–21.
[5] S. Guerra-Gomes, N. Sousa, L. Pinto, J.F. Oliveira, Functional roles of astrocyte calcium elevations: from synapses to behavior, Front. Cell. Neurosci. 11 (January) (2018) 1–7.
[6] S.H. Appel, D.R. Beers, J.S. Henkel, T cell-microglial dialogue in Parkinson's disease and amyotrophic lateral sclerosis: are we listening? Trends Immunol. 31 (1) (2010) 7–17.
[7] C. Acosta, H.D. Anderson, C.M. Anderson, Astrocyte dysfunction in Alzheimer disease, J. Neurosci. Res. 95 (12) (2017) 2430–2447.
[8] D. Boison, C. Steinhäuser, Epilepsy and astrocyte energy metabolism, Glia 66 (6) (2017) 1235–1243.
[9] M.M. Halassa, T. Fellin, P.G. Haydon, The tripartite synapse : roles for gliotransmission in health and disease, Trends Mol. Med. 13 (2) (2006) 54–63.
[10] A. Araque, V. Parpura, R.P. Sanzgiri, P.G. Haydon, Tripartite synapses: glia, the unacknowledged partner, Trends Neurosci. 22 (5) (1999) 208–215.
[11] N.J. Allen, C. Eroglu, Cell biology of astrocyte-synapse interactions, Neuron 96 (3) (2017) 697–708.
[12] M.J. Berridge, J.N. Fain, Inhibition of phosphatidylinositol synthesis and the inactivation of calcium entry after prolonged exposure of the blowfly salivary gland to 5-hydroxytryptamine, Biochem. J. 178 (1) (1979) 59–69.
[13] I. Parker, I. Ivorra, Localized all-or-none calcium liberation by inositol Trisphosphate, Science (80-.) 250 (4983) (1990) 977–979.
[14] C.W. Taylor, S.C. Tovey, IP(3) receptors: toward understanding their activation, Cold Spring Harb. Perspect. Biol. 2 (12) (2010) 1–22.
[15] M.B. Robinson, J.G. Jackson, Astroglial glutamate transporters coordinate excitatory Signaling and brain energetics, Neurochem. Int. 98 (2016) 56–71.
[16] S. Duan, C.M. Anderson, B.A. Stein, R.A. Swanson, Glutamate induces rapid upregulation of astrocyte glutamate transport and cell-surface expression of GLAST, J. Neurosci. 19 (23) (1999) 10193–10200.
[17] S. Takahashi, B.F. Driscoll, M.J. Law, L. Sokoloff, Role of sodium and potassium ions in regulation of glucose metabolism in cultured astroglia, Proc. Natl. Acad. Sci. 92 (1995) 4616–4620.
[18] W.J. Nett, S.H. Oloff, K.D. McCarthy, Hippocampal astrocytes *in situ* exhibit calcium oscillations that occur independent of neuronal activity, J. Neurophysiol. 87 (1) (2002) 528–537.
[19] M. Taheri, G. Handy, A. Borisyuk, J.A. White, Diversity of evoked astrocyte Ca2+ dynamics quantified through experimental measurements and mathematical Modeling, Front. Syst. Neurosci. 11 (October) (2017) 1–19.
[20] F. Aguado, J.F. Espinosa-Parrilla, M.A. Carmona, E. Soriano, Neuronal activity regulates correlated network properties of spontaneous calcium transients in astrocytes *in situ*, J. Neurosci. 22 (21) (2002) 9430–9444.
[21] V. Parpura, A. Schousboe, A. Verkhratsky, Glutamate and ATP at the interface of metabolism and signaling in the brain, Adv. Neurobiol. 11 (2014).
[22] H.R. Parri, V. Crunelli, The role of Ca2+ in the generation of spontaneous astrocytic Ca2+ oscillations, Neuroscience 120 (2003) 979–992.
[23] Y.-X. Li, J. Rinzel, Equations for InsP3 receptor-mediated [Ca2+]i oscillations derived from a detailed kinetic model: a Hodgkin-Hudley like formalism, J. Theor. Biol. 166 (1994) 461–473.
[24] I. Bezprozvanny, J. Watras, B.E. Ehrlich, Bell-shaped calcium-response curves of ins (1,4,5)P3 and calcium-gated channels from endroplasmic reticulum of cerebellum, Nature 351 (6329) (1991) 751–754.
[25] L. Venance, N. Stella, J. Glowinski, C. Giaume, Mechanism involved in initiation and propagation of receptor-induced intercellular calcium signaling in cultured rat astrocytes, J. Neurosci. 17 (6) (1997) 1981–1992.
[26] G.W. De Young, J. Keizer, A single-pool inositol 1,4,5-trisphosphate-receptor-based model for agonist-stimulated oscillations in Ca2+ concentration, Proc. Natl. Acad. Sci. 89 (October) (1992) 9895–9899.
[27] M.J. Rebecchi, S.N. Pentyala, Structure, function, and control of phosphoinositide-specific phospholipase C, Physiol. Rev. 80 (4) (2000) 1291–1335.
[28] V. Allen, P. Swigart, R. Cheung, S. Cockcroft, M. Katan, Regulation of inositol lipid-specific phospholipase c delta by changes in Ca2+ ion concentrations, Biochem. J. 327 (1997) 545–552.
[29] T. Höfer, L. Venance, C. Giaume, Control and plasticity of intercellular calcium waves in astrocytes: a modeling approach, J. Neurosci. 22 (12) (2002) 4850–4859.
[30] G. Dupont, C. Erneux, Simulations of the effects of inositol 1,4,5-trisphosphate 3-kinase and 5-phosphatase activities on Ca2+ oscillations, Cell Calcium 22 (5) (1997) 321–331.
[31] Y. Bernardinelli, P.J. Magistretti, J.-Y. Chatton, Astrocytes generate Na+ −mediated metabolic waves, Proc. Natl. Acad. Sci. 101 (41) (2004) 14937–14942.
[32] P. Bezzi, G. Carmignoto, L. Pasti, S. Vesce, D. Rossi, B.L. Rizzini, T. Pozzant, A. Volterra, Prostaglandins stimulate calcium-dependent glutamate release in astrocytes, Nature 391 (6664) (1998) 281–285.
[33] L. Pellerin, P.J. Magistretti, Glutamate uptake into astrocytes stimulates aerobic glycolysis: a mechanism coupling neuronal activity to glucose utilization, PNAS 91 (October) (1994) 10625–10629.
[34] P. Bezzi, V. Gundersen, J.L. Galbete, G. Seifert, C. Steinhäuser, E. Pilati, A. Volterra,

Astrocytes contain a vesicular compartment that is competent for regulated exocytosis of glutamate, Nat. Neurosci. 7 (6) (2004) 613–620.
[35] P. Lecca, M. Lecca, Mechanistic models of astrocytic glucose metabolism calibrated on PET images, Biomechanics of Cells and Tissues, 2013, pp. 131–155.
[36] P.J. Magistretti, I. Allaman, Lactate in the brain: from metabolic end-product to signalling molecule, Nat. Rev. Neurosci. 19 (4) (2018) 235–249.
[37] M. Lavrentovich, S. Hemkin, A mathematical model of spontaneous calcium(II) oscillations in astrocytes, J. Theor. Biol. 251 (4) (2008) 553–560.
[38] A. Tashiro, J. Goldberg, R. Yuste, Calcium oscillations in neocortical astrocytes under epileptiform conditions, J. Neurobiol. 50 (1) (2002) 45–55.
[39] A.H. Cornell-Bell, S.M. Finkheiner, M.S. Cooper, S.J. Smith, Glutamate induces calcium waves in cultured astrocytes: long-range glial signaling, Science (80-.) 247 (4941) (1990) 470–473.
[40] S. Kirischuk, L. Héja, J. Kardos, B. Billups, Astrocyte sodium signaling and the regulation of neurotransmission, Glia 64 (2016) 1655–1666.
[41] J. Lytton, M. Westlin, S.E. Burk, G.E. Shull, D.H. MacLennan, Functional comparisons between isoforms of the sarcoplasmic or endoplasmic reticulum family of calcium pumps, J. Biol. Chem. 267 (20) (1992) 14483–14489.
[42] M. Falcke, Reading the patterns in living cells —the physics of Ca2 + signaling, Adv. Phys. 53 (3) (2004) 255–440.
[43] M. De Pittà, M. Goldberg, V. Volman, H. Berry, E. Ben-Jacob, Glutamate regulation of calcium and IP3 oscillating and pulsating dynamics in astrocytes, J. Biol. Phys. 35 (4) (2009) 383–411.